

Theoretical study of the dipole-bound anion (H₂O...NH₃)⁻

Cite as: J. Chem. Phys. **108**, 6303 (1998); <https://doi.org/10.1063/1.476037>

Submitted: 03 September 1997 . Accepted: 13 January 1998 . Published Online: 05 August 1998

Piotr Skurski, and Maciej Gutowski



View Online



Export Citation

ARTICLES YOU MAY BE INTERESTED IN

[Theoretical study of the dipole-bound anion \(HF\)₂⁻](#)

The Journal of Chemical Physics **107**, 2968 (1997); <https://doi.org/10.1063/1.474654>

[Theoretical study of the dipole-bound anion \(HPPH₃\)⁻](#)

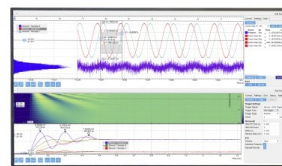
The Journal of Chemical Physics **110**, 274 (1999); <https://doi.org/10.1063/1.478062>

[Vibronic effects in the photon energy-dependent photoelectron spectra of the CH₃CN⁻ dipole-bound anion](#)

The Journal of Chemical Physics **104**, 6976 (1996); <https://doi.org/10.1063/1.471415>

Challenge us.

What are your needs for
periodic signal detection?



Zurich
Instruments



Theoretical study of the dipole-bound anion ($\text{H}_2\text{O}\dots\text{NH}_3$)⁻

Piotr Skurski

Department of Chemistry, University of Gdańsk, 80-952 Gdańsk, Poland

Maciej Gutowski^{a)}

Solid State Theory Group, Materials and Chemical Sciences, Pacific Northwest National Laboratory, Richland, Washington 99352 and Department of Chemistry, University of Utah, Salt Lake City, Utah 84112

(Received 3 September 1997; accepted 13 January 1998)

The adiabatic electron detachment energy for ($\text{H}_2\text{O}\dots\text{NH}_3$)⁻ has been found to be 109 cm^{-1} at the coupled-cluster level of theory with single, double, and noninteractive triple excitations (CCSD(T)), to be compared with the recent experimental result of $123\text{--}129\text{ cm}^{-1}$ obtained by Abdoul-Carime *et al.* [Z. Phys. D **40**, 55 (1997)]. The stationary points on the potential energy surface of the neutral and anionic dimer have been determined at the second-order Møller-Plesset level of theory. Our results indicate that the second-order dispersion interaction between the loosely bound electron and electrons of the neutral dimer is as important as the electrostatic electron-dipole stabilization. The higher-order electron correlation corrections are also very important and the CCSD(T) electron binding energy is approximately four times larger than the Koopmans theorem estimation. In addition, the hydrogen bond in $\text{H}_2\text{O}\dots\text{NH}_3$ is susceptible to a deformation upon attachment of an electron. This deformation enhances both the electrostatic and dispersion components of the electron binding energy. The calculated Franck-Condon factors indicate that neutral dimers formed in electron photodetachment experiments may be vibrationally excited in both soft intermolecular and stiff intramolecular modes. The theoretical photoelectron spectrum based on the calculated Franck-Condon factors is reported. © 1998 American Institute of Physics.

[S0021-9606(98)01315-4]

I. INTRODUCTION

It is well known that individual molecules of neither water nor ammonia can bind an excess electron to form an electronically bound anionic state. Their dimer, however, does bind an electron as has been experimentally demonstrated by Desfrancois *et al.*¹ and Abdoul-Carime *et al.*² in electron transfer collisions between cold water/ammonia clusters and laser-excited Rydberg atoms. Their recent experimental electron affinities, deduced from either formation rates or field-detachment curves, are in the $123\text{--}129\text{ cm}^{-1}$ range.²

The bound anionic states formed by small polar clusters are usually classified as “dipole-bound” because binding of the excess electron is due to the electrostatic dipole potential of the underlying neutral cluster.³ Indeed, it has been shown that any neutral molecule with a dipole moment greater than 1.625 D possesses an infinite number of bound anionic states within the Born-Oppenheimer (BO) approximation.^{4–7} Jordan and Luken demonstrated that the loosely bound electron (*lbe*) in a dipole-bound state occupies a diffuse orbital localized mainly at the positive side of the molecular dipole.⁸ The role of non-BO effects has been studied by Garrett, who concluded that they are negligible for dipole bound states with E_{bind} 's much larger than molecular rotational constants.⁹

The simplest theoretical approach to estimate E_{bind} of a dipole-bound anion is based on Koopmans' theorem (KT).¹⁰ The KT binding energy (E_{bind}^{KT}) is given by the negative of

the energy of the relevant unfilled orbital obtained from a Hartree-Fock self-consistent field (SCF) calculation on the neutral molecule. This is a static approximation which neglects both electron correlation and orbital relaxation effects. Orbital relaxation effects have been found to be quite small for a variety of dipole-bound anionic states.^{11–19} On the other hand, the role of electron correlation effects has proven to be more controversial. Early studies of polar diatomics^{20,21} and simple polar organic molecules¹² indicated that electron correlation effects played only a small role in electron binding to these species. However, electron correlation effects were found to cause a significant destabilization of the dipole-bound anion of nitromethane.²² In contrast, we have found that inclusion of electron correlation effects leads to a sizable stabilization of the dipole-bound anions of HCN, CH_3CN , C_3H_2 , C_4H_2 , C_5H_2 , uracil, $(\text{HF})_n$ ($n=2,3$), $(\text{H}_2\text{O})_2$, and $(\text{HCN})_2$,^{13–19} and another theoretical study on the dipole-bound anion of nitromethane confirmed this observation.²³ We concluded that the electron correlation contribution to E_{bind} encompasses: (i) a stabilizing dynamical correlation between the *lbe* and the electrons of the neutral molecule, and (ii) the change of the electrostatic stabilization due to improved description of the charge distribution of the neutral. Furthermore, we found that electron correlation effects beyond the second-order Møller-Plesset (MP2) level contribute substantially to the stability of dipole-bound anionic states and solvated electrons.^{13–19}

For many years a dipole-bound anion was regarded as being an unperturbed neutral molecule with the excess distant electron tethered to the dipole.³ Our recent results for

^{a)}Corresponding author (PNNL).

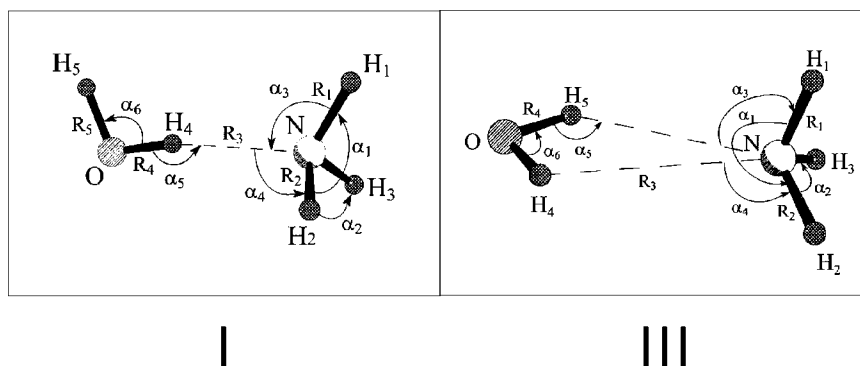


FIG. 1. Internal coordinates for the neutral and anionic $\text{H}_2\text{O}\dots\text{NH}_3$ used in the present work.

$(\text{HF})_2$, $(\text{HF})_3$, and $(\text{H}_2\text{O})_2$ indicate, however, that hydrogen bonds in polar clusters are susceptible to a deformation upon attachment of an electron.^{15–19} Moreover, we have demonstrated that vibrational structure displayed in the photoelectron spectrum of $(\text{HF})_2^-$ and $(\text{H}_2\text{O})_2^-$ may be explained through Franck-Condon (FC) factors without invoking the resonant and vibronic effects, which may be important for rigid dipole-bound anions such as CH_3CN^- .²⁴

Analysis of rate constants for the formation of $(\text{H}_2\text{O}\dots\text{NH}_3)^-$ in Rydberg electron transfer experiments suggested that the neutral complex and the anion have essentially the same geometry.² This finding was confirmed in density functional calculations but the calculated electron binding energy of ca. 300 cm^{-1} was much larger than the experimental result.²

The neutral $\text{H}_2\text{O}\dots\text{NH}_3$ complex has been studied both experimentally^{25–28} and theoretically.^{29–31} An equilibrium C_s structure with H_2O as a proton donor and slightly non-linear hydrogen bond was deduced from microwave and far-infrared spectra.^{25,27} The dipole moment deduced from the Stark effect for the microwave and radio frequency spectra is in the 3.2–3.9 D range²⁵ and the significant uncertainty results from a limited knowledge of the component of the dipole moment which is perpendicular to the a molecular axis.^{25,27}

The potential energy surface of the neutral $\text{H}_2\text{O}\dots\text{NH}_3$ has been explored by Yeo and Ford at the MP2/6-31G** level.²⁹ They characterized three C_s symmetry stationary points with NH_3 as a proton acceptor. Two of these structures, labeled **I** and **III**, are characterized on Fig. 1. They also considered structure **II**, which differs from structure **I** by a rotation of NH_3 around the hydrogen bond by 180° . Another structure with H_2O as a proton acceptor collapsed to structure **III** in the course of geometry optimization. In their calculations at the MP2/6-31G** level, Yeo and Ford found structure **II** to be a minimum, while structure **I** was characterized as a transition state, but the difference in energy between these structures was only 3.5 cm^{-1} . The bifurcated structure **III** was characterized at the RHF/6-31G** level as a transition state, with the energy higher by 18 kJ/mol than the energy at stationary points **I** and **II**.

In this work we present highly correlated *ab initio* calculations for the neutral and the anion of $\text{H}_2\text{O}\dots\text{NH}_3$. We studied differences in potential energy surfaces of the neutral

and anionic dimer at the MP2 level of theory and we calculated FC factors for the formation of vibrationally excited neutral dimers in a photoelectron spectroscopy experiment. A model theoretical spectrum based on the calculated FC factors was also produced. The electron binding energy was determined at the coupled-cluster level of theory with single, double, and noninteractive triple excitations (CCSD(T)).³²

II. METHODS TO CALCULATE E_{bind}

The calculated values of E_{bind} were obtained using a supermolecular approach, i.e., by subtracting the energies for the anion from those of the neutral. This approach requires the use of size-extensive methods and we have employed the MP perturbation theory up to the fourth order and the CCSD(T) method.³² In addition, E_{bind} was analyzed within a perturbation framework designed for dipole-bound anions and solvated electrons.¹⁷

In the perturbation scheme,¹⁷ we consider a neutral molecule (N) and the lbe as weakly interacting species and we follow the analogy with the theory of intermolecular interactions^{33,34} to analyze E_{bind} in terms of physically meaningful components. The total electronic Hamiltonian for the anion is partitioned into H^0 , which corresponds to the Hartree-Fock level of theory for N and the KT level of theory for the lbe , and two perturbations, W^N and V^{lbe} :

$$H = H^0 + \lambda W^N + \eta V^{lbe}, \quad (1)$$

where the formal expansion parameters λ and η are introduced to define the perturbation theory orders and have physical values equal to unity. The zeroth-order Hamiltonian

$$H^0 = F^N + F^{lbe} \quad (2)$$

is the sum of Fock operators for all electrons in the anion and every Fock operator is determined by the occupied orbitals of N . The fluctuation operator for the neutral molecule, W^N , results from Møller-Plesset partitioning of the electronic Hamiltonian of N , and the fluctuation-interaction operator V^{lbe} has the form

$$V^{lbe} = \sum_{i \in N} \frac{1}{r_{lbe,i}} - (J_N(lbe) - K_N(lbe)), \quad (3)$$

where $r_{lbe,i}$ is the distance between the i -th electron of N and the lbe , and J_N and K_N are respectively the Coulomb and exchange operators for N .

On applying double-perturbation theory³³ to Hamiltonian (1) one obtains the perturbation expansion for the anion energy

$$E = \sum_{k=0}^{\infty} \sum_{l=0}^{\infty} \epsilon^{(kl)}, \quad (4)$$

where $\epsilon^{(kl)}$ is of the k -th order in W^N and l -th order in V^{lbe} . The sum of the three lowest-order terms reproduces the SCF energy of N and E_{bind}^{KT} :

$$\epsilon^{(00)} + \epsilon^{(10)} + \epsilon^{(01)} = E_N^{SCF} - E_{bind}^{KT}. \quad (5)$$

E_{bind}^{KT} takes into account the Coulomb and exchange interaction between the lbe and the SCF charge distribution of N . This is a static approximation which neglects both orbital relaxation and electron correlation effects.

The non-KT contributions to E_{bind} are given by other $\epsilon^{(kl)}$ terms with $l \geq 1$. The term $\epsilon^{(02)}$ separates into the induction and dispersion contributions^{33,34}

$$\epsilon^{(02)} = \epsilon_{ind}^{(02)} + \epsilon_{disp}^{(02)}. \quad (6)$$

These contributions are invariant with respect to a unitary transformation of the occupied orbitals which describe N . The term $\epsilon_{ind}^{(02)}$ describes polarization of N by the lbe and, as an orbital relaxation effect, is reproduced when E_{bind} is obtained from the difference in the SCF energies of the neutral and anionic species

$$\Delta E_{bind}^{SCF-ind} = E_{bind}^{SCF} - E_{bind}^{KT} \approx -\epsilon_{ind}^{(02)}, \quad (7)$$

where

$$E_{bind}^{SCF} = E_N^{SCF} - E_A^{SCF} \quad (8)$$

and E_A^{SCF} stands for the SCF energy of the anion. In fact, the term $\Delta E_{bind}^{SCF-ind}$ includes not only the static polarization of N by the lbe but also the secondary effect of backpolarization. The term $\Delta E_{bind}^{SCF-ind}$ is expected to grow with increasing polarizability of N and with decreasing average separation between the lbe and N .

The term $\epsilon_{disp}^{(02)}$ describes a dynamical correlation between the lbe and the electrons of N . This stabilizing effect, brought by quantum mechanical charge fluctuations, may be very important for weakly bound anions in view of a significant polarizability of the lbe . The term $\epsilon_{disp}^{(02)}$ is approximated here by $\Delta E_{bind}^{MP2-disp}$, which takes into account proper permutational symmetry for all electrons in the anion

$$\epsilon_{disp}^{(02)} \approx \sum_{a \in N} \sum_{r < s} \frac{|\langle \phi_a \phi_{lbe} | | \phi_r \phi_s \rangle|^2}{e_a + e_{lbe} - e_r - e_s} = -\Delta E_{bind}^{MP2-disp}, \quad (9)$$

where ϕ_a and ϕ_{lbe} are spin orbitals occupied in the zeroth-order wave function, ϕ_r and ϕ_s are unoccupied orbitals, and e 's are the corresponding orbital energies. Very similar values of $\Delta E_{bind}^{MP2-disp}$ are obtained using the SCF orbitals of N or those of A , and the results reported in this work are obtained using the orbitals of the anion.

Higher-order corrections to E_{bind} cannot be neglected. First, there are higher-order corrections in V^{lbe} given by the $\epsilon^{(0l)}$ ($l > 2$) terms. Second, there are corrections $\epsilon^{(kl)}$ for $k, l \neq 0$ which contribute to E_{bind} not only through V^{lbe} but also through W^N . It is well established that electron correlation affects the static charge distribution of N and leads to a discrepancy between the SCF and correlated dipole moments of polar molecules. Therefore, the static Coulomb interaction between the lbe and the SCF charge density of N , which is contained in E_{bind}^{KT} , has to be rectified and the first correction of this type is contained in the MP2 electron binding energy.³⁴

The MP2 contribution to E_{bind} defined as

$$\Delta E_{bind}^{MP2} = E_{bind}^{MP2} - E_{bind}^{SCF} \quad (10)$$

is naturally split into the dispersion and non-dispersion terms

$$\Delta E_{bind}^{MP2} = \Delta E_{bind}^{MP2-disp} + \Delta E_{bind}^{MP2-no-disp} \quad (11)$$

with the latter dominated by $\epsilon^{(21)}$.³⁴ The higher-order MP contributions to E_{bind} are defined as

$$\Delta E_{bind}^{MPn} = E_{bind}^{MPn} - E_{bind}^{MP(n-1)}, \quad n = 3, 4. \quad (12)$$

Finally, the contributions beyond the fourth-order are estimated by subtracting MP4 results from those obtained at the coupled-cluster level

$$\Delta E_{bind}^{CC} = E_{bind}^{CC} - E_{bind}^{MP4}. \quad (13)$$

In particular, the DQ, SDQ, and SDTQ MP4 energies are subtracted from the D, SD, and SD(T) coupled-cluster binding energies,³² respectively.

III. COMPUTATIONAL DETAILS

The $1s$ orbitals of oxygen and nitrogen were excluded from the electron correlation treatments. All electronic structure results reported in this study were obtained with the Gaussian 94 program.³⁵

The diffuse character of the lbe (see Fig. 2) necessitates the use of extra diffuse functions with very low exponents.⁸ In addition, the initial basis set chosen to describe the neutral molecular host should be flexible enough to: (i) accurately describe the static charge distribution of the neutral, and (ii) allow for polarization of the neutral upon electron attachment and for the dispersion stabilization. The majority of our calculations were performed with the aug-cc-pVDZ basis set³⁶ supplemented with diffuse s , p , d and sometimes f functions. The extra diffuse s and p functions always share the exponent values. The results presented below justify our basis set selection.

First, we explored dependence of E_{bind} on the choice of the extra diffuse functions. These tests were performed with the aug-cc-pVDZ core basis set, with only the extra diffuse functions being varied. We have used an even-tempered six term spd basis set, with the lowest exponent equal to 9.0 (-6) a.u. and the geometric progression ratio equal to 5.0 for each angular momentum. The extra diffuse functions were centered on the nitrogen atom, at the positive end of molecular dipole. Next, we tested that the MP2 electron binding energy increases by less than 1 cm^{-1} after inclusion

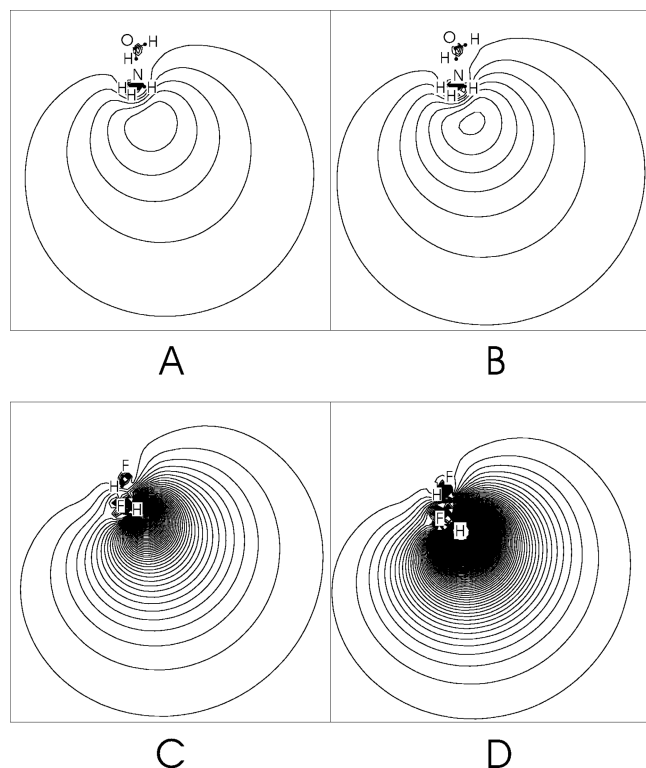


FIG. 2. Contour plot of the density of the loosely bound electron in $(\text{H}_2\text{O}\dots\text{NH}_3)^-$ for the equilibrium geometry of the neutral (A) and anionic (B) dimer. The separation between contour lines is $0.000002 e/\text{\AA}^3$. The density distribution for the *lbe* in $(\text{HF})_2^-$ for the equilibrium geometry of the neutral (C) and anionic (D) dimer is also presented with the same contour line separation as for $(\text{H}_2\text{O}\dots\text{NH}_3)^-$.

of a six term set of diffuse *f* functions and by less than 1 cm^{-1} when the six term *spd* set is replaced by the seven term *sp* and eight term *d* diffuse sets with the geometric progression ratio reduced to 3.2.³⁷ The *sp*-only diffuse set recovers more than 92% of E_{bind} at the MP2 level. Moreover, the equilibrium structure of the neutral dimer is practically the same with the *sp* and *spd* diffuse sets. Therefore, the diffuse *d* functions were omitted from the basis set when

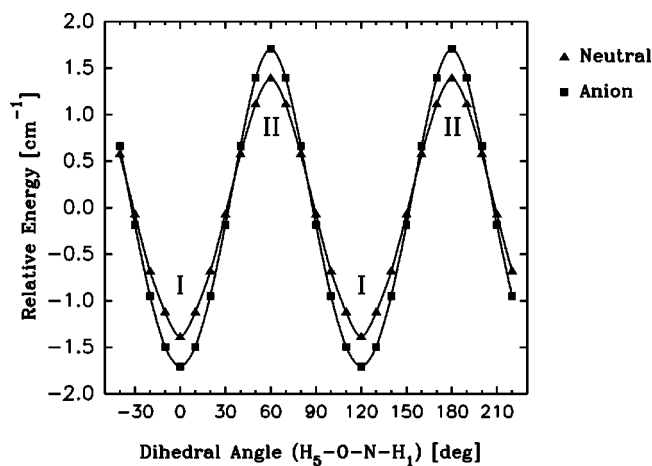


FIG. 3. The MP2 energy profile for a rotation of the NH_3 and H_2O moieties around the hydrogen bond.

carrying out the MP2 geometry optimizations and the frequency calculations.

We have also explored the dependence of E_{bind} on the core basis set chosen to describe the neutral molecular host. The MP2 values of E_{bind} obtained with Sadlej's medium-size polarized basis set³⁸ and Dunning's aug-cc-pVTZ set,³⁶ with the six term *spd* diffuse set fixed, differ by less than 1 and 2 cm^{-1} , respectively, from the aug-cc-pVDZ results. We believe that our MP2 electron binding energies obtained with the aug-cc-pVDZ basis set supplemented with the six term *spd* diffuse set are underestimated by less than 5% due to basis set incompleteness effects.

We have studied the dependence of the dipole moment of the neutral complex on geometrical displacements induced by electron attachment. Both SCF and MP2 values of the dipole moment are reported; the latter were obtained with the generalized density corresponding to the second-order energy.³⁹

The FC factors, i.e., the squares of overlap integrals between vibrational wave functions of the neutral and anionic dimer, were calculated in harmonic approximation at the MP2 level. Both geometrical equilibrium parameters as well as curvatures of the potential energy surface are modified upon attachment of a distant electron and the resultant FC factors may contribute to vibrational structure in a photoelectron spectrum. The polyatomic FC factors were calculated using Doktorov and co-workers' recursion relations⁴⁰ as implemented in the code of Ref. 41 and assuming the temperature of 10 K in the mass selected ion beam.⁴² The intensity for the 0-0 transition was normalized to one and all other intensities were scaled accordingly. The notation n_k^l used in Sec. IV C means that for the *n*-th mode there is an excitation from *k* to *l* quanta and 0_0^0 stands for the 0-0 transition.

IV. RESULTS

The relevant rotational energy level spacings for the water-ammonia dimer are much smaller than the calculated values of E_{bind} . Hence, non-BO coupling between the electronic and rotational degrees of freedom is expected to be of secondary importance for this dipole-bound anion and is not considered in this study.

A. MP2 geometries and harmonic frequencies

We have explored the MP2 potential energy surfaces of the neutral and anionic dimer and we have determined stationary points corresponding to structures **I**–**III**. In contrast to the conclusions of Yeo and Ford,²⁹ structure **I** for the neutral was characterized as a minimum whereas structure **II** as a transition state with an imaginary frequency of $23i \text{ cm}^{-1}$ along an *a''* mode, which corresponds to a rotation of the NH_3 and H_2O moieties around the hydrogen bond. For the anion, the imaginary frequency is even larger and amounts to $35i \text{ cm}^{-1}$. The barrier for the rotation of NH_3 around the hydrogen bond is only 3.0 and 3.4 cm^{-1} for the neutral and the anion, respectively (see Fig. 3). The experimental estimation of this barrier height in the neutral complex is $10.5 \pm 5.0 \text{ cm}^{-1}$,²⁵ which confirms that the barrier is very small. The dipole moments of **I** and **II** differ by less than 0.02 D, and the values of E_{bind}^{MP2} differ by 0.5 cm^{-1} . With a

TABLE I. Geometries and harmonic vibrational frequencies for the neutral and dipole-bound anionic state of (H₂O...NH₃) at their **I** and **III** stationary points. Frequencies in cm⁻¹, distances in Å, angles in degrees, dipole moment μ of the neutral dimer in D, ^y zero-point vibrational energies in kcal/mol.

System	Geometry		$\mu_{neutral}$		Frequencies		E_0^{vib}
			SCF	MP2			
(H ₂ O...NH ₃) Structure I	$R_1=1.020$ $R_3=1.968$ $R_5=0.965$ $\alpha_1=106.41$ $\alpha_3=121.02$ $\alpha_5=170.26$	$R_2=1.020$ $R_4=0.979$ $\alpha_2=106.24$ $\alpha_4=107.95$ $\alpha_6=104.44$	3.66	3.54	$\omega_1(a'')=11^a$ $\omega_3(a'')=178^c$ $\omega_5(a'')=447^e$ $\omega_7(a'')=1110^g$ $\omega_9(a'')=1648^i$ $\omega_{11}(a'')=3479^k$ $\omega_{13}(a'')=3630^m$ $\omega_{15}(a'')=3895^p$	$\omega_2(a')=173^b$ $\omega_4(a')=200^d$ $\omega_6(a')=728^f$ $\omega_8(a')=1645^h$ $\omega_{10}(a')=1662^j$ $\omega_{12}(a')=3578^l$ $\omega_{14}(a')=3633^n$	37.181
(H ₂ O...NH ₃) ⁻ Structure I	$R_1=1.020$ $R_3=1.959$ $R_5=0.965$ $\alpha_1=106.18$ $\alpha_3=119.01$ $\alpha_5=173.56$	$R_2=1.020$ $R_4=0.980$ $\alpha_2=106.22$ $\alpha_4=109.25$ $\alpha_6=104.17$	3.79	3.66	$\omega_1(a'')=22^a$ $\omega_3(a'')=187^c$ $\omega_5(a'')=449^e$ $\omega_7(a'')=1111^g$ $\omega_9(a'')=1648^i$ $\omega_{11}(a'')=3475^k$ $\omega_{13}(a'')=3626^m$ $\omega_{15}(a'')=3892^p$	$\omega_2(a')=181^b$ $\omega_4(a')=198^d$ $\omega_6(a')=741^f$ $\omega_8(a')=1644^h$ $\omega_{10}(a')=1667^j$ $\omega_{12}(a')=3553^l$ $\omega_{14}(a')=3627^n$	37.175
(H ₂ O...NH ₃) Structure III	$R_1=1.021$ $R_3=2.708$ $\alpha_1=105.99$ $\alpha_3=106.68$ $\alpha_5=113.88$	$R_2=1.021$ $R_4=0.967$ $\alpha_2=105.73$ $\alpha_4=101.28$ $\alpha_6=100.27$	4.09	3.90	$\omega_1(a'')=320i^b$ $\omega_3(a'')=118^q$ $\omega_5(a'')=182^s$ $\omega_7(a'')=1093^g$ $\omega_9(a'')=1650^j$ $\omega_{11}(a'')=3475^k$ $\omega_{13}(a'')=3626^n$ $\omega_{15}(a'')=3915^x$	$\omega_2(a'')=21^a$ $\omega_4(a'')=129^f$ $\omega_6(a'')=452^l$ $\omega_8(a'')=1630^u$ $\omega_{10}(a'')=1652^v$ $\omega_{12}(a'')=3625^m$ $\omega_{14}(a'')=3816^w$	36.287
(H ₂ O...NH ₃) ⁻ Structure III	$R_1=1.021$ $R_3=2.693$ $\alpha_1=105.74$ $\alpha_3=107.08$ $\alpha_5=113.99$	$R_2=1.021$ $R_4=0.967$ $\alpha_2=105.48$ $\alpha_4=101.36$ $\alpha_6=100.00$	4.12	3.93	$\omega_1(a'')=324i^b$ $\omega_3(a'')=124^q$ $\omega_5(a'')=188^s$ $\omega_7(a'')=1096^g$ $\omega_9(a'')=1649^j$ $\omega_{11}(a'')=3471^k$ $\omega_{13}(a'')=3620^n$ $\omega_{15}(a'')=3909^x$	$\omega_2(a'')=24^a$ $\omega_4(a'')=141^f$ $\omega_6(a'')=462^l$ $\omega_8(a'')=1626^u$ $\omega_{10}(a'')=1651^v$ $\omega_{12}(a'')=3619^m$ $\omega_{14}(a'')=3812^w$	36.301

^aTwisting intermolecular mode.

^bWater and ammonia rocking (intermolecular mode).

^cNH₂H₃ twisting and OH₄...N bending (intermolecular mode).

^dN...H₄ (hydrogen bond) stretching (intermolecular mode).

^eH₂O rocking/in-plane bending of hydrogen bond (intermolecular mode).

^fOH₄ bending/out-of-plane bending of hydrogen bond (intermolecular mode).

^gUmbrella inversion mode in ammonia.

^hH₂O scissors and H₂NH₃ scissors, dominated by the motion of atoms belonging to ammonia monomer.

ⁱNH₃ bending dominated by the H₁ motion.

^jH₂O scissors and H₂NH₃ scissors, dominated by the motion of atoms belonging to water monomer.

^kIn-phase NH stretching.

^lIn-phase OH stretching dominated by the H₄ motion.

^mOut-of-phase NH₂ and NH₃ stretching.

ⁿIn-phase NH₂ and NH₃ stretching plus NH₁ stretching out-of-phase to NH₂ and NH₃.

^oOH₅ stretching.

^pHydrogen bond stretching (intermolecular mode).

^qNH₃ wagging/in-plane bending of hydrogen bond (intermolecular mode).

^rNH₃ and H₂O rocking/out-of-plane bending of hydrogen bond (intermolecular mode).

^sNH₂O wagging (intermolecular mode).

^tH₂O scissors.

^uH₂NH₃ scissors.

^vIn-phase OH stretching.

^wOut-of-phase OH stretching.

^yMP2 results obtained with the aug-cc-pVDZ basis set supplemented with the 6sp diffuse set.

limited accuracy of electronic structure methods and basis sets in mind, we have decided to pursue a detailed analysis of E_{bind} for structure **I** but the results for structure **II** are expected to be very similar.

The bifurcated structure **III** proved to be a transition

state for both the neutral and the anion with a frequency of 320i and 324i cm⁻¹, respectively, along an a'' mode (a rocking vibration of the H₂O monomer); see Table I. The MP2 energy of **III** was found to be 152 and 156 meV higher than the energy of **I** for the anion and the neutral, respectively.

The dipole moments of the H₂O and NH₃ moieties are nearly parallel in **III** and a significant dipole moment of the neutral complex is anticipated. Therefore, we have also selected **III** for further analysis of E_{bind} . One should keep in mind, however, that the value of E_{bind} for **III** ought to be considered as a theoretical upper limit for this complex.

Our rotational constant A for the neutral complex **I** amounts to 4.93 cm⁻¹ and agrees well with the findings of Stockman *et al.*²⁵ which are 4.93 and 4.92 cm⁻¹ for the para and ortho tunneling state, respectively. Our MP2 constant (B+C)/2 amounts to 6283.2 MHz and is slightly larger than the experimental values.^{25,27} Our equilibrium N-O distance is 2.938 Å and it is shorter by 0.05 Å than the experimental value.^{25,27} Notice that the latter was obtained with structures of the monomers assumed to be unchanged upon complexation and may correspond to a vibrationally averaged value. The MP2 value of the α_5 parameter, reported in Table I, indicates that the hydrogen bond is bent by 9.7 deg which is in excellent agreement with the non-linearity of 10 deg in the neutral complex suggested by Stockman *et al.*²⁵

Our results for the neutral species reported in Table I may be also compared with the theoretical results of Yeo and Ford.²⁹ The agreement is to 0.008 Å and 0.5 deg for the intramonomer parameters. The hydrogen-bonded fragment of the system seems to be more sensitive to the basis set employed and these geometrical parameters differ by as much as 0.02 Å and 5 deg. The frequencies corresponding to intramonomer modes are systematically smaller than those calculated by Yeo and Ford at the MP2/6-31G** level whereas those of intermolecular modes agree to 20 cm⁻¹. Our harmonic MP2 frequencies are systematically larger than the experimental fundamentals.^{28,26} The latter, however, strongly depend on the matrix used to form the dimer.

The potential energy surfaces of the neutral and anionic dimer differ only slightly (see Table I). These small geometrical distortions are, however, sufficient to increase the dipole moment, μ , of the neutral by 0.12 and 0.03 D for **I** and **III**, respectively, at the MP2 level. The SCF dipole moment of the neutral dimer follows the same trend but it is larger than the MP2 result by 0.12 and 0.19 D for **I** and **III**, respectively. The increase of the dipole moment upon electron attachment leads to a contraction of the *lbe* density; see Fig. 2 in which the *lbe* charge distributions for (H₂O...NH₃)⁻ and (HF)₂⁻ are presented at the anionic and neutral equilibrium geometries. The contraction for (H₂O...NH₃)⁻ is, however, smaller than for (HF)₂⁻, for which the dipole moment of the neutral complex increases by 0.47 D upon electron attachment.¹⁶

The electron attachment leads to a shortening of the hydrogen bond length (R_3) by ca. 0.01 Å for both structures. The most affected angles are those involved in the hydrogen bond, i.e., α_3 , α_4 , and α_5 which are modified by a few degrees for structure **I**. The changes of geometrical parameters are generally smaller for structure **III** than for **I**. The A rotational constant for structure **I** decreases by 0.05 cm⁻¹ upon electron attachment and the (B+C)/2 constant increases by 18 MHz.

The normal vibrational modes are characterized in Table I, where the harmonic MP2 frequencies are also reported.

TABLE II. Incremental electron binding energies (in cm⁻¹) for dipole-bound anionic state of the water-ammonia complex.

Component	Structure I ^a	Structure I ^b	Structure III ^c	Structure III ^d
E_{bind}^{KT}	19.4	24.9	39.0	40.9
(E_{IP}^{KT})	(20.8)	(26.8)	(42.1)	(44.2)
$\Delta E_{bind}^{SCF-ind}$	0.7	0.9	1.5	1.6
$\Delta E_{bind}^{MP2-disp}$	23.7	29.8	45.0	47.0
$\Delta E_{bind}^{MP2-no-disp}$	-5.9	-7.4	-14.0	-14.6
ΔE_{bind}^{MP3}	-0.1	-0.1	0.4	0.4
ΔE_{bind}^{MP4}	5.2	6.4	8.3	8.6
$\Delta E_{bind}^{CCSD(T)}$	49.4	56.0	71.6	73.3
Sum	92.4	110.5	151.9	157.3

^{a,c}For the geometry of the neutral.

^{b,d}For the geometry of the anion.

For both structures, the geometrical relaxation in the dimer upon electron attachment is primarily along the first three a' modes. These modes are associated with the in-plane rotation of both monomers and the intermolecular hydrogen bond stretching. For both structures, the frequencies of soft intermolecular modes are usually increased upon electron attachment and the largest shift by 13 cm⁻¹ is for the third a'' mode in structure **I** (an out-of-plane bending of the hydrogen bond). The frequencies of the stiff intramonomer stretching modes are usually decreased and the largest shift by -25 cm⁻¹ is reported for the twelfth mode in structure **I**, which describes primarily the stretching of the O-H₄ bond. Due to cancellation of the inter and intramonomer contributions, the change of the total zero-point vibrational energy upon electron attachment is small and at the MP2 level amounts to -2 and 5 cm⁻¹ for **I** and **III**, respectively.

B. Electron binding energies

The electron binding energy was partitioned into incremental contributions calculated at "successive" levels of theory (KT, SCF, MP n ($n=2,3,4$), and CCSD(T)), and the results for structures **I** and **III** are presented in Table II. In the KT approximation, the electron binding energy results from the electrostatic and exchange interactions of the extra electron with the SCF charge distribution of the neutral molecule. The distribution is primarily characterized by the dipole moment, but interactions with higher permanent multipoles as well as penetration effects are also taken into account. The values of E_{bind}^{KT} correlate well with the SCF dipole moment for the neutral complex (see Fig. 4). They are larger for structure **III** than for structure **I**, and for both structures they are slightly larger for the anionic than for the neutral equilibrium geometry.

In Table II we also presented the KT predictions of the ionization potential for (H₂O...NH₃)⁻, which are labeled E_{IP}^{KT} . It is well known that ionization potentials are usually better reproduced at the KT level than electron affinities due to a partial cancellation of orbital relaxation and electron correlation corrections.²⁰ The differences between E_{bind}^{KT} and E_{IP}^{KT} are very small for this system, which indicates that orbital relaxation effects upon electron attachment are also very small. We prefer to start our analysis of electron bind-

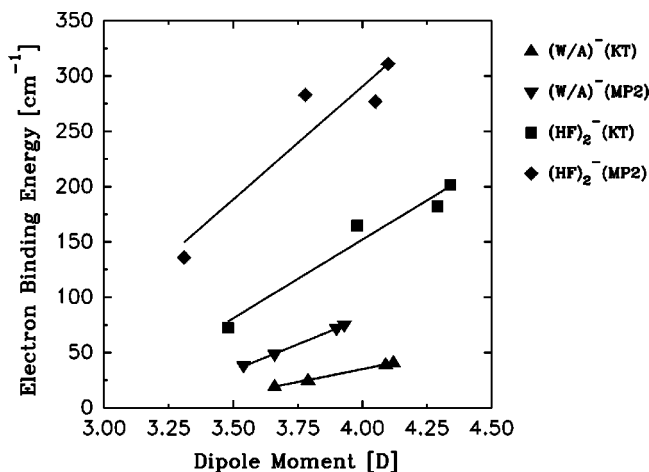


FIG. 4. Dependence of E_{bind}^{KT} (E_{bind}^{MP2}) on the SCF (MP2) dipole moments of the neutral $\text{H}_2\text{O}\dots\text{NH}_3$ and $(\text{HF})_2$ complexes.

ing energies in weakly bound anions from E_{bind}^{KT} rather than from E_{IP}^{KT} because the former is reproduced at the lowest level of the perturbation scheme; see Eq. 5.

The SCF binding energies include orbital relaxation and thus take into account static polarization of the neutral molecule by the *lbe* and the secondary effect of backpolarization. The values of the orbital relaxation correction to E_{bind}^{KT} , denoted $\Delta E_{bind}^{SCF-ind}$ in Table II, are of little importance and do not exceed 2 cm^{-1} . The effect is larger for **III** than for **I** because the former has a larger dipole moment, the *lbe* is closer to the molecular core, and may exert a larger induction effect. Similarly, $\Delta E_{bind}^{SCF-ind}$ is larger for the anionic than for the neutral geometry, for both **I** and **III**.

The term $\Delta E_{bind}^{MP2-disp}$ results from a dynamical correlation between the *lbe* and the electrons of the neutral molecule. This stabilizing effect is larger in magnitude than E_{bind}^{KT} for all geometries considered; see Table II. This finding is consistent with our earlier results for other dipole-bound anions^{13–19} and has important implications for model potentials designed to describe dipole-bound anions and solvated electrons.^{43,44} For structure **I**, the value of $\Delta E_{bind}^{MP2-disp}$ increases from 23.7 cm^{-1} at the optimal geometry of the neutral to 29.8 cm^{-1} at the optimal geometry of the anion. The mechanism for this increase is probably similar as that for the SCF induction effect: The less distant *lbe* has a stronger dispersion interaction with the neutral core.

In addition to the dispersion interaction, electron correlation also affects the charge distribution of the neutral molecule and its electrostatic interaction with the *lbe*. This effect first appears at the MP2 level and is approximated by $\Delta E_{bind}^{MP2-no-disp}$. The values of $\Delta E_{bind}^{MP2-no-disp}$ are destabilizing and correlate with the MP2 correction to the dipole moment of the complex; see Table I.

The values of E_{bind}^{MP2} are approximately twice as large as the values of E_{bind}^{KT} and the dispersion stabilization is the main source of the discrepancy. It is then quite interesting that the values of E_{bind}^{MP2} correlate well with the MP2 values of dipole moment for the neutral complex (see Fig. 4). The slope of E_{bind} with respect to μ is, however, different for the MP2 and KT methods.

TABLE III. Contributions of various classes of excitations to E_{bind} (cm^{-1}) at the anionic equilibrium geometries from Table I.

Method	Structure I		Structure III	
	E_{bind}	ΔE_{bind}	E_{bind}	ΔE_{bind}
UMP4(DQ)	46.9	-1.2	73.4	-2.0
UMP4(SDQ)	51.7	3.6	80.3	4.9
UMP4(SDTQ)	54.5	6.4	84.0	8.6
CCD	46.4	-0.5	72.7	-0.7
CCSD	97.0	45.3	141.7	61.4
CCSD(T)	110.5	56.0	157.3	73.3
T4(CCSD)	—	26.5	—	34.5
T5(CCSD)	—	-12.9	—	-18.9

The convergence of the MP series for the electron binding energy in $(\text{H}_2\text{O}\dots\text{NH}_3)^-$ is slow. The contribution from ΔE_{bind}^{MP3} is negligible, that from ΔE_{bind}^{MP4} represents ca. 6% of E_{bind} , and higher-order electron correlation effects, approximated here by $\Delta E_{bind}^{CCSD(T)}$ (the difference in the CCSD(T) and MP4 binding energies), are one order of magnitude larger than ΔE_{bind}^{MP4} .

The contributions to ΔE_{bind}^{MP4} and $\Delta E_{bind}^{CCSD(T)}$ from various classes of excitations are collected in Table III and will be discussed in detail for the anionic geometry of structure **I**. The MP4 contribution from double and quadruple excitations, $\Delta E_{bind}^{MP4(DQ)}$ is destabilizing and amounts to -1.2 cm^{-1} . The contributions from single excitations, given by the difference between $\Delta E_{bind}^{MP4(SDQ)}$ and $\Delta E_{bind}^{MP4(DQ)}$, is stabilizing and equal to 4.8 cm^{-1} , whereas that from triple excitations, given by the difference between $\Delta E_{bind}^{MP4(SDTQ)}$ and $\Delta E_{bind}^{MP4(SDQ)}$, is also stabilizing and equal to 2.8 cm^{-1} . The final fourth-order contribution $\Delta E_{bind}^{MP4(SDTQ)}$ amounts to 6.4 cm^{-1} .

The effects of single and triple excitations are magnified by one order of magnitude in the framework of coupled-cluster methods. The contribution from single excitations, calculated as the difference between E_{bind}^{CCSD} and E_{bind}^{CCD} , amounts to 50.6 cm^{-1} . The CCSD(T) contribution from triple excitations, calculated as the difference between $E_{bind}^{CCSD(T)}$ and E_{bind}^{CCSD} , contains the fourth-order contribution with the CCSD amplitudes and a fifth-order term,³² which are labeled T4(CCSD) and T5(CCSD), respectively, in Table III. The fourth-order contribution with the CCSD amplitudes is stabilizing and amounts to 26.5 cm^{-1} . The fifth-order contribution, however, is destabilizing and amounts to -12.9 cm^{-1} , leading to the total stabilizing contribution from triple excitations of 13.5 cm^{-1} .

Higher-than-fourth-order electron correlation contributions to E_{bind} may also be extracted from the data collected in Table III. The difference between E_{bind}^{CCD} and $E_{bind}^{MP4(DQ)}$ is small and amounts to -0.5 cm^{-1} . However, when single excitations are included the situation is quite different; indeed the difference between E_{bind}^{CCSD} and $E_{bind}^{MP4(SDQ)}$ amounts to 45.3 cm^{-1} . Finally, the value of $\Delta E_{bind}^{CCSD(T)}$ amounts to 56.0 cm^{-1} and represents 51% of $E_{bind}^{CCSD(T)}$.

The results discussed above indicate that the MP4 treatment of electron correlation effects is not sufficient for this dipole-bound anion. The role of single excitations is ex-

tremely important and may be related to the fact that the charge distribution of the *lbe* is seriously modified when the neutral molecular core is modified by electron correlation effects. This is indicated by the fact that the largest CCSD amplitudes correspond to single excitations from the orbital occupied by the *lbe*. It may well be that physical interpretation of E_{bind} calculated in coupled-cluster framework would benefit if Brueckner orbitals³² were used to construct the single determinantal wave functions of the anion and the neutral. In addition, the contribution from triple excitations proved to be very sensitive to the form of amplitudes of the single and double excitations. For this dipole-bound anion it may be necessary to adopt methods such as CCSDT-1 or CCSDT, which treat high-order correlation effects more accurately than does the CCSD(T) method.³²

The convergence of electron binding energy with respect to the level of electron correlation treatment is quite similar for $(\text{H}_2\text{O}\dots\text{NH}_3)^-$ and $(\text{HF})_2^-$.¹⁶ The magnitude of electron binding energy is, however, much larger in $(\text{HF})_2^-$. This can be hardly explained by a larger dipole moment (see Fig. 4). For the anionic minimum energy structures, the MP2 electron binding energy is six times larger for $(\text{HF})_2^-$ whereas the MP2 dipole moment is only 0.12 D larger for $(\text{HF})_2$ than for $\text{H}_2\text{O}\dots\text{NH}_3$. For $(\text{HF})_2$, the dependence of E_{bind}^{MP2} on μ^{MP2} is not monotonic and the ‘‘slope’’ is larger than for $\text{H}_2\text{O}\dots\text{NH}_3$. These results indicate that a physical model of a dipole-bound anion can not be solely based on the dipole moment of the neutral molecular host. Perusal of the data presented in Table II and in Ref. 16 indicates that low order contributions to E_{bind} , such as E_{bind}^{KT} and ΔE_{bind}^{MP2} , are particularly different in $(\text{H}_2\text{O}\dots\text{NH}_3)^-$ and $(\text{HF})_2^-$. These differences may result from a different charge distribution of the *lbe* in $(\text{H}_2\text{O}\dots\text{NH}_3)^-$ and $(\text{HF})_2^-$ (see Fig. 2) and the less distant *lbe* in $(\text{HF})_2^-$ may interact more strongly with the neutral host. We speculate that the more compact charge distribution of the *lbe* in $(\text{HF})_2^-$ results not only from a larger dipole moment but also from unusually small occupied orbital exclusion effects.

C. Photoelectron spectrum

To the best of our knowledge, the photoelectron spectrum of $(\text{H}_2\text{O}\dots\text{NH}_3)^-$ has not been recorded yet. The photoelectron spectra of similar systems, such as $(\text{HF})_2^-$ and $(\text{H}_2\text{O})_2^-$, displayed a vibrational structure which intrigued experimentalists for some time.^{3,42} Both FC factors¹⁶ as well as resonant and vibronic effects²⁴ were invoked to explain these features.

In Section IV A we reported differences in potential energy surfaces of the neutral and anionic dimer. Both geometrical parameters and curvatures of the potential energy surface were slightly modified upon attachment of a distant electron. Therefore, we calculated FC factors using the MP2 geometrical Hessians and the C_s equilibrium geometries of structure I. The position of the 0-0 transition transition, 109 cm^{-1} , was determined from the difference in the CCSD(T) energy of $(\text{H}_2\text{O}\dots\text{NH}_3)$ and $(\text{H}_2\text{O}\dots\text{NH}_3)^-$ at their respective MP2 minimum geometries (107 cm^{-1}) and corrected for the difference in the zero-point vibrational en-

TABLE IV. Theoretical values of Franck-Condon factors and transition energies (cm^{-1}) in the photoelectron spectrum of $(\text{H}_2\text{O}\dots\text{NH}_3)^-$.

Transition	Position	FC factor	Intensity
0_0^0	109	1.000	1.000
1_0^0	131	0.364	0.364
1_0^4	153	0.199	0.199
$1_0^1 1_0^0$	142	0.256	0.010
$1_0^2 1_0^0$	304	0.004	0.004
$1_0^2 1_0^1 1_0^1$	3783	0.001	0.001
$1_0^3 1_0^0$	298	0.002	0.002
$1_0^3 1_0^1$	321	0.002	0.002
$1_0^4 1_0^0$	331	0.004	0.004
$1_0^1 1_0^3 1_0^0$	3750	0.003	0.003
$1_0^1 1_0^3 1_0^1$	3772	0.003	0.003
2_0^0	282	0.012	0.012
$2_0^1 1_0^1 1_0^0$	3761	0.004	0.004
$3_0^1 1_0^0$	265	0.052	0.002
$3_0^1 1_0^1 1_0^0$	1935	0.002	0.002
4_0^0	309	0.012	0.012
$4_0^1 1_0^1 1_0^0$	3788	0.002	0.002
5_0^0	557	0.002	0.002
$5_0^1 1_0^2 1_0^0$	4135	0.001	0.001
$5_0^1 1_0^5 1_0^0$	4452	0.001	0.001
$13_0^1 1_0^1 1_0^0$	3717	0.033	0.001

ergy (2 cm^{-1}) determined at the MP2 level. The agreement with the experimental electron binding energy of 123–129 cm^{-1} (Ref. 2) is remarkable.

The values of FC factors reported in Table IV indicate that many vibrationally excited levels of the neutral dimer may be populated in the electron photodetachment experiment. There are many transitions which involve the first a'' mode associated with the rotation of the NH_3 and H_2O moieties around the hydrogen bond. The curvature for this mode increases four times upon electron attachment which leads to numerous non-zero FC factors for overtones, combination bands, and hot band transitions. The pseudorotation around the hydrogen bond may indeed be different in the anion than in the neutral complex (see Fig. 3) but our FC factors, obtained in the harmonic approximation, should be considered cautiously in view of the small magnitude of the rotation barrier.

The calculated FC factors were convoluted with Gaussian line shapes (fwhm=218 cm^{-1} ,⁴²) and the resulting theoretical spectrum is shown in Fig. 5. The 0_0^0 and 1_0^2 transitions are separated by only 22 cm^{-1} . Furthermore, there are also the 1_0^4 and $1_0^5 1_0^1$ transitions separated from the 0_0^0 transition by 44 and 33 cm^{-1} , respectively. Therefore the resulting theoretical peak has a maximum at 121 cm^{-1} and fwhm of 228 cm^{-1} . Many combination bands contribute to a higher energy peak with the maximum at 3760 cm^{-1} and the intensity of 0.01.

V. CONCLUSIONS

The electron correlation effects contribute 77% to the electronic stability of the anion of $\text{H}_2\text{O}\dots\text{NH}_3$. The second-order dispersion stabilization is as important as the electrostatic stabilization due to the SCF dipole of the neutral dimer but the largest electron correlation effect results from higher-

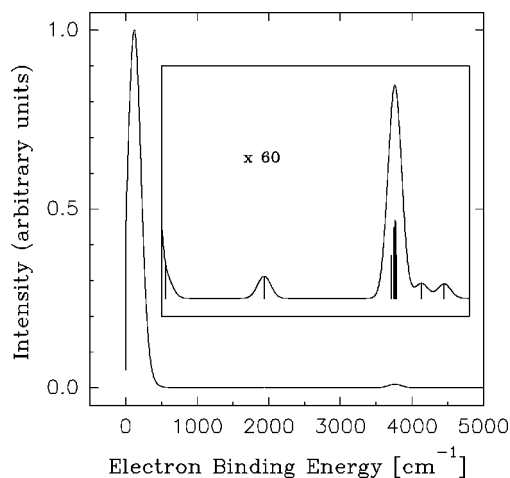


FIG. 5. Theoretical photoelectron spectrum of $(\text{H}_2\text{O}\dots\text{NH}_3)^-$ based on calculated Franck-Condon factors.

than-fourth-order terms. The single and triple excitations proved to be much more important in the CCSD(T) than in the MP4 approach.

The hydrogen bond in $\text{H}_2\text{O}\dots\text{NH}_3$ is susceptible to a deformation upon attachment of a distant electron. The minor geometrical deformation is accompanied by an enhancement of the dipole moment of the neutral cluster and by enlargement of the electrostatic, dispersion, and induction components of the electron binding energy.

The differences in the potential energy surfaces of the neutral and anionic dimer lead to many non-zero Franck-Condon factors which may be responsible for a weak vibrational structure in the photoelectron spectrum of $(\text{H}_2\text{O}\dots\text{NH}_3)^-$.

ACKNOWLEDGMENTS

We would like to acknowledge support of this work by the Division of Geosciences and Engineering and the Division of Chemical Sciences both of the Office of Basic Energy Sciences, and the Office of Energy Research of the US Department of Energy. Some of computational resources were provided by the National Energy Research Scientific Computing (NERSC) facility at Lawrence Berkeley National Laboratory. This work was performed in part under auspices of the U.S. Department of Energy, under Contract No. DE-AC6-76RLO 1830, with Battelle Memorial Institute, which operates the Pacific Northwest National Laboratory. Partial supports by the NSF Grant No. CHE-9116286, the Polish State Committee for Scientific Research (KBN) Grant No. BW/8000-5-0186-7, and a computer time grant from the Utah Supercomputing Institute are also gratefully acknowledged. P.S. is a holder of a research grant of the Foundation of Polish Science (FNP).

- ¹C. Desfrancois, B. Baillon, J. P. Schermann, S. T. Arnold, J. H. Hendricks, and K. H. Bowen, *Phys. Rev. Lett.* **72**, 48 (1994).
- ²H. Abdoul-Carime, A. Wakisaka, Y. Bouteiller, C. Desfrancois, and J. P. Schermann, *Z. Phys. D* **40**, 55 (1997).
- ³A. W. Castleman, Jr. and K. H. Bowen, Jr., *J. Phys. Chem.* **100**, 12911 (1996).
- ⁴E. Fermi and E. Teller, *Phys. Rev.* **72**, 399 (1947).
- ⁵A. S. Wightman, *Phys. Rev.* **77**, 521 (1950).
- ⁶J. M. Levy-Leblond, *Phys. Rev.* **153**, 1 (1967).
- ⁷M. H. Mittleman and V. P. Myerscough, *Phys. Lett.* **23**, 545 (1966).
- ⁸K. D. Jordan and W. Luken, *J. Chem. Phys.* **64**, 2760 (1976).
- ⁹W. R. Garrett, *J. Chem. Phys.* **77**, 3666 (1982).
- ¹⁰T. Koopmans, *Physica (Amsterdam)* **1**, 104 (1934).
- ¹¹G. L. Gutsev, A. L. Sobolewski, and L. Adamowicz, *Chem. Phys.* **196**, 1 (1995).
- ¹²G. L. Gutsev and L. Adamowicz, *J. Phys. Chem.* **99**, 13412 (1995).
- ¹³M. Gutowski, P. Skurski, A. I. Boldyrev, J. Simons, and K. D. Jordan, *Phys. Rev. A* **54**, 1906 (1996).
- ¹⁴K. Yokoyama, G. W. Leach, J. B. Kim, W. C. Lineberger, A. I. Boldyrev, and M. Gutowski, *J. Chem. Phys.* **105**, 10706 (1996).
- ¹⁵M. Gutowski, P. Skurski, J. Simons, and K. D. Jordan, *Int. J. Quantum Chem.* **64**, 183 (1997).
- ¹⁶M. Gutowski and P. Skurski, *J. Chem. Phys.* **107**, 2968 (1997).
- ¹⁷M. Gutowski and P. Skurski, *J. Phys. Chem. B* **101**, 9143 (1997).
- ¹⁸M. Gutowski, K. D. Jordan, and P. Skurski, *J. Phys. Chem.* (in press).
- ¹⁹M. Gutowski and P. Skurski (unpublished).
- ²⁰J. Simons and K. D. Jordan, *Chem. Rev.* **87**, 535 (1987).
- ²¹L. Adamowicz and R. J. Bartlett, *J. Chem. Phys.* **88**, 313 (1988).
- ²²L. Adamowicz, *J. Chem. Phys.* **91**, 7787 (1989).
- ²³G. L. Gutsev and R. J. Bartlett, *J. Chem. Phys.* **105**, 8785 (1996).
- ²⁴C. G. Bailey, C. E. H. Dessent, M. A. Johnson, and K. H. Bowen, Jr., *J. Chem. Phys.* **104**, 6976 (1996).
- ²⁵P. A. Stockman, R. E. Bumgarner, S. Suzuki, and G. A. Blake, *J. Chem. Phys.* **96**, 2496 (1992).
- ²⁶A. Engdahl and B. Nelander, *J. Chem. Phys.* **91**, 6604 (1989).
- ²⁷P. Herbine and T. R. Dyke, *J. Chem. Phys.* **83**, 3768 (1985).
- ²⁸B. Nelander and L. Nord, *J. Phys. Chem.* **86**, 4375 (1982).
- ²⁹G. A. Yeo and T. A. Ford, *Can. J. Chem.* **69**, 632 (1991).
- ³⁰Z. Latajka and S. Scheiner, *J. Phys. Chem.* **94**, 217 (1990).
- ³¹J. D. Dill, L. C. Allen, W. C. Topp, and J. A. Pople, *J. Am. Chem. Soc.* **97**, 7220 (1975).
- ³²R. J. Bartlett, J. F. Stanton, in *Reviews in Computational Chemistry*, Vol. V, edited by K. B. Lipkowitz and D. B. Boyd (VCH, New York, 1994).
- ³³B. Jeziorski, R. Moszynski, and K. Szalewicz, *Chem. Rev.* **94**, 1887 (1994).
- ³⁴G. Chałasiński, M. M. Szczęśniak, *Chem. Rev.* **94**, 1723 (1994).
- ³⁵Gaussian 94, Revision B.1, M. J. Frisch *et al.* (Gaussian, Inc., Pittsburgh PA, 1995).
- ³⁶R. A. Kendall, T. H. Dunning, Jr., and R. J. Harrison, *J. Chem. Phys.* **96**, 6796 (1992).
- ³⁷M. Gutowski and J. Simons, *J. Chem. Phys.* **93**, 3874 (1990).
- ³⁸A. J. Sadlej, *Theor. Chim. Acta* **79**, 123 (1991).
- ³⁹K. B. Wiberg, C. M. Hadd, T. J. LePage, C. M. Breneman, and M. J. Frisch, *J. Phys. Chem.* **96**, 671 (1992).
- ⁴⁰E. V. Doktorov, I. A. Malkin, and V. I. Man'ko, *J. Mol. Spectrosc.* **64**, 302 (1977); **56**, 1 (1975).
- ⁴¹D.-S. Yang, M. Z. Zgierski, D. M. Rayner, P. A. Hackett, A. Martinez, D. R. Salahub, P.-N. Roy, and T. Carrington, Jr., *J. Chem. Phys.* **103**, 5335 (1995).
- ⁴²J. H. Hendricks, H. L. de Clercq, S. A. Lyapustina, and K. H. Bowen, Jr., *J. Chem. Phys.* **107**, 2962 (1997).
- ⁴³C. Desfrancois, *Phys. Rev. A* **51**, 3667 (1995).
- ⁴⁴R. N. Barnett, U. Landman, S. Dhar, N. R. Kestner, J. Jortner, and A. Nitzan, *J. Chem. Phys.* **91**, 7797 (1989).